NRC Research Press

ARTICLE

Flexural ductility of reinforced concrete beams with lap-spliced bars

Mehrollah Rakhshanimehr, M. Reza Esfahani, M. Reza Kianoush, B. Ali Mohammadzadeh, and S. Roohollah Mousavi

Abstract: In this paper, the flexural ductility of lap-spliced reinforced concrete (RC) beams is experimentally investigated. Twenty-four specimens were designed and manufactured for laboratory experiments. Concrete compressive strength, amount of transverse reinforcement over the splice length, and the diameter of longitudinal bars were selected as the main variables. The ductility of tested specimens is evaluated based on a previously defined ductility ratio. Results show that concrete strength and amount of transverse reinforcement over the splice have major effects on ductility. With an appropriate amount of transverse reinforcement, a satisfactory ductility response for different concrete strengths can be obtained. The CSA-A23.3-04 Standard provisions on bond strength and ductility of lap-spliced RC beams are evaluated and discussed. This study shows that the provisions in predicting the bond strength of lap-spliced concrete beams are adequate but may not achieve a satisfactory performance for ductility. An equation is proposed to achieve the appropriate ductility.

Key words: bond, ductility, longitudinal tensile reinforcement, reinforced concrete beam, splice length, transverse reinforcement.

Résumé : Cet article présente une étude expérimentale sur la ductilité en flexion de poutres en béton armé à recouvrement. Un total de 24 spécimens a été conçu et fabriqué pour des expériences en laboratoire. Les principales variables sont la résistance en compression du béton, la quantité d'armature transversale sur la longueur du recouvrement et le diamètre des tiges longitudinales. La ductilité des échantillons testés est évaluée en se basant selon un rapport de ductilité prédéfini. Les résultats montrent que la résistance du béton et la quantité d'armature transversale du recouvrement ont un impact sur la ductilité. Avec une armature transversale adéquate, nous obtenons une réponse en ductilité satisfaisante pour différentes résistances de béton. Les dispositions de la norme CSA A23.3-04 sur la résistance des liens et la ductilité des poutres en béton armé à recouvrement sont évaluées et discutées. La présente étude montre que les dispositions servant à prédire la résistance du lien de poutres en béton armé à recouvrement sont adéquates mais pourraient ne pas atteindre un niveau de rendement adéquat en ductilité. Une équation est proposée afin d'atteindre la ductilité adéquate. [Traduit par la Rédaction]

Mots-clés : lien, ductilité, armature en tension longitudinale, poutre en béton armé, longueur de recouvrement, armature transversal.

Introduction

Bond between concrete and the tensile reinforcement is a major problem in reinforced concrete (RC) structures, as far as strength and safety is concerned. The bond strength of spliced bars in concrete depends on several factors such as surface deformation of reinforcing bars, embedment length, bar diameter, confinement, concrete strength, environment conditions, and loading conditions (Rezansoff et al. 1997; Aly 2007). Because of the complexity and the effect of a variety of parameters, researchers have not been able to include theoretically all parameters in their solutions for bond phenomena. They rather have tried experimental solutions by trial and error procedures and engineering judgment to overcome the problem.

Transverse reinforcement confines developed and spliced bars by limiting the progression of splitting cracks and, thus, increases the bond strength and resists prying effects in flexure (Tepfers 1973; Orangun et al. 1977). Based on the results of different series of experimental works, Orangun et al. (1977) proposed an empirical equation for bond strength prediction. The equation later became the basis of ACI Committee 318 (1995) equation for the bond strength of spliced bars. The Canadian Standard CSA-A23.3-04 used a similar equation for bond strength prediction. In later studies, it was found that although the ACI Committee 318 (1995) equation is quite conservative in estimating the bond strength of spliced bars, it fails to satisfy the ductility requirement of the flexural beams (Azizinamini et al. 1999*a*). The ductility requirement of flexural beams is satisfied when the reinforcing bar ratio ρ is less than the maximum value, ρ_{max}. The ductility of spliced-beams tested by Azizinamini et al. (1999*a*) was significantly less than that of similar flexural beams without spliced bars having the same reinforcing bar ratios. It was observed that the failure of these beams is brittle without exhibiting ductility (Azizinamini et al. 1999*a*). Azizinamini et al. (1999*b*) proposed some modifications to ACI Committee 318 (1995) equation for lap-spliced high strength RC beams. Azizinamini et al. (1999*a*, 1999*b*) also showed that the available code provisions do not satisfy the ductility requirement for lap-spliced RC beams. They concluded that some transverse reinforcement should be provided over the splice length, so that the ductility response of these beams is improved. Esfahani (2000) discussed the results obtained by Azizinamini et al. (1999*a*) and proposed a modification for the

Received 16 February 2013. Accepted 13 May 2014.

M. Rakhshanimehr, M.R. Esfahani, and B.A. Mohammadzadeh. Department of Civil Engineering, Ferdowsi University of Mashhad, Mashhad, Iran.
M.R. Kianoush. Department of Civil Engineering, Ryerson University, Toronto, M5B 2K3 Ontario, Canada.
S.R. Mousavi. Department of Civil Engineering, University of Sistan and Baluchestan, Zahedan, Iran.
Corresponding author: M. Reza Kianoush (e-mail: kianoush@ryerson.ca).

Fig. 1. Definition of displacement–ductility ratio.

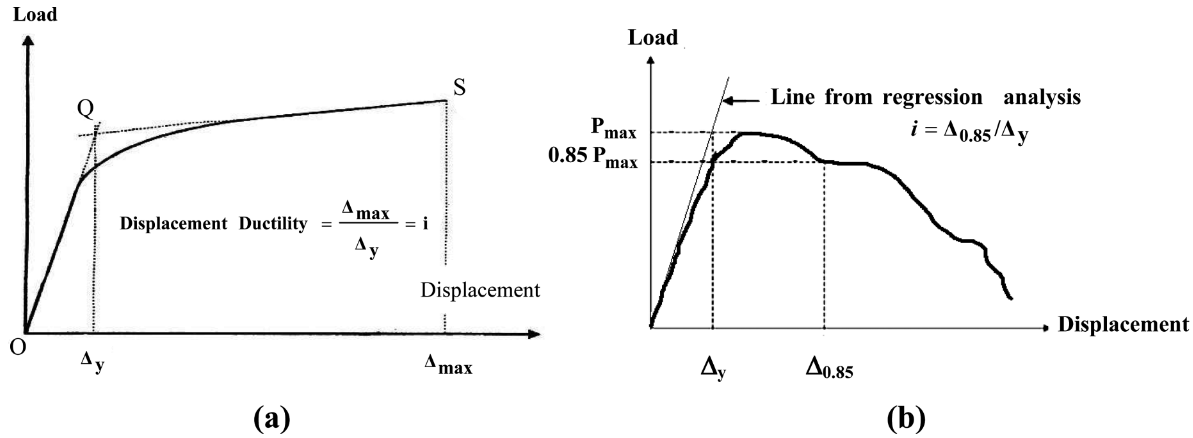

ductility criteria of lap-spliced high strength concrete beams. Esfahani and Rangan (1998*a*, 1998*b*, 2000) proposed equations from the results of several experiments to consider the effect of different parameters (i.e., concrete cover, concrete strength, development and splice lengths, the size and rib properties of deformed bars, transverse reinforcement, and the spacing of spliced bars) on bond strength of lap-spliced RC beams. Later, Esfahani and Kianoush (2005) studied the effect of the amount of transverse reinforcement over the splices on the ductility behavior of beams. They found that the bond strength and ductility are not necessarily increased by increasing the splice length (l_d), especially in the case of high strength concrete beams. On the other hand, they concluded that by providing an appropriate amount of transverse reinforcement, a significant increase in bond strength and ductility can be obtained.

A displacement ductility ratio was selected as an index by Azizinamini et al. (1999*a*) to assess the ductility of lap-spliced RC beam specimens. This index is defined as the ratio of the maximum mid-span displacement over the first yield displacement of beams (eq. (1)). The first yield displacement, Δ_y, corresponds to the intersection of the tangents to the load displacement curve at the origin and maximum displacement, Δ_{max} (Fig. 1*a*). Therefore, the use of displacement–ductility ratio presents a new criterion in addition to the strength criterion for predicting the behavior of lap-spliced reinforced concrete beams.

$$i = \frac{\Delta_{max}}{\Delta_y} \tag{1}$$

In their studies, Azizinamini et al. (1999*a*) showed that although some specimens had splice length more than that required by the ACI Committee 318 (1995) equation and satisfied the strength criterion of $u_{test}/u_{ACI} > 1$, the specimens failed in a very brittle and violent manner without exhibiting ductility. This was attributed to a lack of transverse reinforcement used over the splices.

Cohn and Bartlett (1982) proposed a relatively more appropriate definition for a displacement ductility index. Based on their definition, the displacement ductility index can be estimated as the ratio of the displacement corresponding to 85% of the maximum load on the post-peak portion of the curve to the displacement corresponding to the first yield displacement of a beam (eq. (2) and Fig. 1*b*).

$$i = \frac{\Delta_{0.85}}{\Delta_c} \tag{2}$$

Pessiki and Pieroni (1997) studied the effect of tie-bars on the ductility of columns made of high strength concrete. They showed that, to achieve a proper ductility, the relation $\rho_s(f_y/f'_c)$ should be kept constant where ρ_s is the ratio of the transverse reinforcement volume to the volume of the concrete core in columns; therefore, if the value of f'_c is increased, the amount of ρ_s should also be increased proportionately. It should be noted that since the displacement at peak load may not represent yielding of reinforcement, the term Δ_c instead of Δ_y is used here.

Recent studies have shown that the design provisions of current codes can evaluate the bond strength of lap-spliced concrete beams with reasonable accuracy. However, they fail to fulfill a satisfactory ductility criterion for these beams. It has been shown that, to improve the ductility response of these beams, some transverse reinforcement should be provided over the splice length. However, the required transverse reinforcement which results in an adequate ductility for the spliced-beams has not been presented. In this research, the splice length and the required transverse reinforcement are determined using the authors' previous proposed equations. Based on the test results of this study, an assessment on strength and ductility of beams is made and compared with the code provisions. In this study, a flexural beam without spliced bars and with a tensile steel ratio less than ρ_{max} is tested as a reference specimen and its ductility behavior is used as a basis for evaluating the ductility of other beam specimens tested with spliced bars.

Theoretical background

Esfahani and Kianoush (2005) proposed the following equation to calculate the splice length, l_d:

$$l_d = \frac{T}{a\sqrt{f'_c}} = \frac{A_b f_s}{a\sqrt{f'_c}} \tag{3}$$

where

$$a = 7.2 d_b \frac{C/d_b + 0.5}{C/d_b + 3.6} \tag{4}$$

In eqs. (3) and (4), A_b is the cross-sectional area of one longitudinal tensile bar in mm²; f_s is the bar tensile stress in MPa; d_b is the tensile bar diameter in mm; l_d is the length of splice in mm; f'_c is the compressive strength of concrete in MPa; C is the minimum of C_x, C_y, and $(C_s + d_b)/2$; C_x and C_y are the side and bottom covers of the reinforcing bars in mm respectively; and C_s is the spacing between spliced bars in mm. For design purposes, the bar tensile stress f_s in eq. (3) can be replaced by the yield strength of the steel reinforcing bars f_y. Equation (3) is valid to calculate the splice length only if the amount of transverse reinforcement calculated by eq. (5) is used over the splice length. According to Esfahani and Kianoush (2005), this amount of transverse reinforcement is necessary to satisfy the ductility requirement of flexural beams.

$$\frac{A_t}{s} = \frac{67C}{f_R A_b}\left\{\frac{1.63M}{[(M+1)(0.88+0.12)\times(C_{Med}/C)]} - 1\right\} \tag{5}$$

In the above equation C_{Med} is the median of C_x, C_y, and $(C_s + d_b)/2$ (Esfahani and Rangan 1998*b*); A_t is the cross-sectional area of one transverse reinforcement; s is the spacing of transverse reinforcement; $f_R = 1$ if $R_r < 0.11$ and $f_R = 1.6$ if $R_r \geq 0.11$; R_r is the relative rib area equal to projected rib area normal to the bar axis/(nominal bar perimeter × centre-to-centre rib spacing); and M is found by eq. (6)

$$M = \mathrm{Cosh}\left(0.0022 l_d \sqrt{3\frac{f'_c}{d_b}}\right) \tag{6}$$

The above equations were derived based on the following equation for bond strength (Esfahani and Rangan 2000; Esfahani and Kianoush 2005).

$$u_{Esf} = \frac{T}{\pi d_b l_d} = u_c \frac{1 + 1/M}{1.85 + 0.024\sqrt{M}}\left(0.88 + 0.12\frac{C_{Med}}{C}\right) \times \left(1 + 0.015 f_R \frac{A_t A_b}{Cs}\right) \tag{7}$$

where u_{Esf} is the proposed bond stress, T is the tensile bar force, and u_c is the maximum local bond stress (MPa) at the time of failure and is found by eq. (8)

$$u_c = 2.7\frac{C/d_b + 0.5}{C/d_b + 3.6}\sqrt{f'_c} \tag{8}$$

According to Canadian Standard Association (CSA-A23.3-04), the development length of reinforcing bars is calculated by the following equation:

$$l_d = 1.15\frac{k_1 k_2 k_3 k_4}{(d_{cs} + K_{tr})}\frac{f_y}{\sqrt{f'_c}}A_b \tag{9}$$

where l_d is the development length of the steel bars, k_1 is the bar location factor, k_2 is the coating factor, k_3 is the concrete density factor, k_4 is the bar size factor, A_b is the bar cross-sectional area, f_y is the yield strength of tensile bar, f'_c is the concrete compressive strength, and d_{cs} is the smaller of the distance from the closest concrete surface to the centre of the bar being developed, or two-thirds the centre-to-centre spacing of bars being developed. The term $(d_{cs} + K_{tr})$ shall not be taken greater than $2.5d_b$. The term K_{tr} is the transverse reinforcement index specified as $K_{tr} = A_{tr}f_{yt}/10.5sn$, where A_{tr} is the area of transverse reinforcement, f_{yt} is the specified yield stress of steel reinforcing bars, s is the centre-to-centre spacing of the transverse reinforcement, and n is the number of bars being developed along the plan of splitting. The splice length for steel bars in tension shall be taken as $1.6l_d$.

Using eq. (9) and $u_{CSA} = A_b f_y/\pi d_b l_d$, the bond strength u_{CSA} (the bond stress calculated by CSA-A23.3-04 Code) can be calculated by eq. (10).

$$u_{CSA} = \frac{(d_{cs} + K_{tr})\sqrt{f'_c}}{1.15 k_1 k_2 k_3 k_4 \pi d_b} \tag{10}$$

Experimental study

Design and construction of lap-spliced RC beam specimens

Materials

Three different longitudinal tensile reinforcing bars with nominal diameters of 20, 22, and 25 mm were used in the specimens. Using the stress versus strain relationship, the yield stress of these reinforcing bars were found to be 460, 440, and 420 MPa, respectively, by a tensile test process. Two specimens were tested for each bar size.

The concrete for beam specimens was provided by a local ready-mix supplier. Different concretes with compressive strength ranging from 22 MPa to 74 MPa were used for the beam specimens. The maximum aggregate size in the mixtures were 25 mm and 12 mm for normal strength concrete (22 MPa to 45 MPa compressive strength) and high strength concrete (70 MPa and 74 MPa compressive strength), respectively. Also, the W/C ratios were 0.50, 0.45, 0.40, and 0.30 for 22 MPa, 31 MPa, 45 MPa, and 70–74 MPa concrete strengths, respectively. The cement contents were 450 kg/m^3 and 520 kg/m^3 for normal strength and high strength concretes, respectively. Silica fume (41.6 kg/m^3) and superplasticizer (4.2 L/m^3) were used in the mixture of high strength concrete.

Test specimens

In the two test series, 24 beam specimens with overall span lengths of 3.3 m (3 m centre-to-centre between the roller supports) with simply supported ends were designed and manufactured. The structural details of specimens are shown in Table 1 and Fig. 2. The clear concrete cover for the longitudinal tensile bars for all specimens was 40 mm. Two top reinforcing bars with a nominal diameter of 12 mm and a nominal cross-sectional area of 113 mm^2 were used for all specimens. The splice lengths and the amount of transverse reinforcement over the splices were calculated based on eqs. (3) and (5), respectively. To verify the expected mode of failure, and to ensure the reliability of the test procedures, construction process and the design calculations of the beams, two initial specimens named B-01 and B-02 reinforced with longitudinal tensile bars with a nominal diameter of 22 mm (nominal cross-sectional area of 380 mm^2) and cross-sectional dimensions of 200 mm × 300 mm were designed, constructed and tested. On this basis, the parameters for the other specimens were carefully selected and the beams were designed. Tensile bars with nominal diameters of 20 and 25 mm (nominal cross-sectional areas of 314 mm^2 and 491 mm^2, respectively) and a revised cross-sectional dimension of 250 mm × 300 mm (for a better construction layout) were selected for specimens B-1 to B-22. Two lap-spliced tensile bars were used for each specimen as shown in Fig. 2. To prevent shear failure in different specimens, adequate transverse reinforcement was provided over the shear span of all specimens. This transverse reinforcement was 12 mm nominal diameter stirrups with 100 mm spacing. The longitudinal bar ratio, $\rho = A_s/bd$ (Table 2), in the beam sections of test series I and II, was considerably less than the maximum ratio, ρ_{max}; A_s is tensile bar area in the section, b is the beam width, and d is the beam effective depth.

In the specimens of test series I including specimens B-1 to B-13, B-01, and B-02 (with the exception of specimen B-14, which had no lap-spliced bars), the variable parameters in the study were the concrete compressive strength f'_c and tensile and transverse bar diameters. To ensure that the longitudinal tensile bars of series I specimens do not reach the yield stress, and to ensure the specimens fail by bond rather than by bending, the length of splices were calculated based on bar tensile stress of 0.8 f_y by eq. (3). The results of this test series was expected to determine the efficiency of the proposed eq. (3) for bond strength prediction. It should be

Table 1. Details of test specimens.

	Specimen group	Test	Bar diameter d_b (mm)	f'_c (MPa)	l_d (mm) eq. (3)	Transverse reinforcement over the splice length
Series I	Initial specimens	B-01	22	24	503	D8@43 mm
		B-02	22	24	503	D12@100 mm
	Group 1	B-1	20	22	402	D8@38 mm
		B-2	20	22	402	D12@86 mm
		B-3	20	45	268	D8@38 mm
		B-4	20	45	268	D12@86 mm
		B-5	20	70	215	D8@38 mm
		B-6	20	70	215	D12@86 mm
	Group 2	B-7	25	22	507	D8@43 mm
		B-8	25	22	507	D12@97 mm
		B-9	25	45	338	D8@43 mm
		B-10	25	45	338	D12@97 mm
		B-11	25	70	271	D8@43 mm
		B-12	25	70	271	D12@97 mm
	Reference specimens	B-13	20	22	402	—
		B-14	20	22	—	—
Series II	Specimens with splice length based on $f_s = f_y$ or $1.3f_y$	B-15	20	31	375	D10@43 mm
		B-16	25	31	518	D10@43 mm
		B-17	20	74	245	D10@43 mm
		B-18	25	74	339	D10@43 mm
		B-19	20	31	468	D10@43 mm
		B-20	25	31	647	D10@43 mm
		B-21	20	74	307	D10@43 mm
		B-22	25	74	424	D10@43 mm

Fig. 2. Dimensions of specimens and reinforcement.

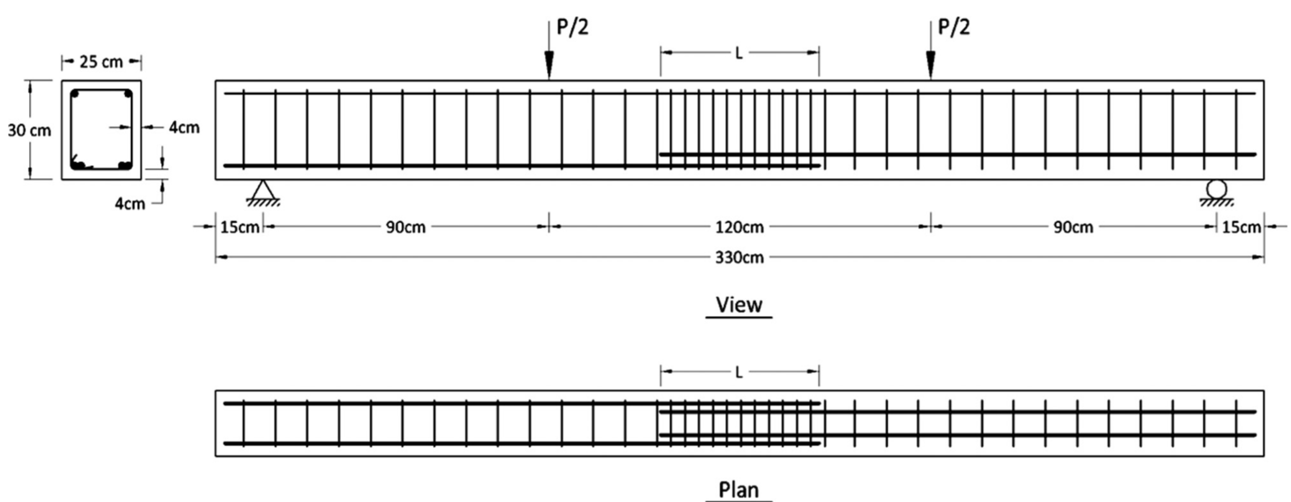

Table 2. Reinforcing bar ratio ρ and the value of parameter j for different parameters in specimens.

d_b (mm)	f'_c (MPa)	A_s (mm²)	ρ	ρ_{max}	E_c (MPa)	n	k*	$j = 1 - k/3$
20	22	628	0.0105	0.0177	22045	9.98	0.3644	0.88
20	45	628	0.0105	0.0317	31528	6.98	0.3161	0.89
20	70	628	0.0105	0.0376	39323	5.59	0.2886	0.90
20	31	628	0.0105	0.0248	26168	8.41	0.3406	0.89
20	74	628	0.0105	0.0378	40430	5.44	0.2853	0.90
25	22	981.25	0.0164	0.0177	22045	9.98	0.431	0.86
25	45	981.25	0.0164	0.0317	31528	6.98	0.3771	0.87
25	70	981.25	0.0164	0.0376	39323	5.59	0.346	0.88
25	31	981.25	0.0164	0.0248	26168	8.41	0.4046	0.87
25	74	981.25	0.0164	0.0378	40430	5.44	0.3422	0.89
22	24	759.88	0.0158	0.0193	23025	9.55	0.4192	0.86
22	24	759.88	0.0158	0.0193	23025	9.55	0.4192	0.86

*$k = \sqrt{2n\rho + (n\rho)^2} - n\rho$ where $n = E_s/E_c$, E_s = 220000 MPa and $E_c = 4700\sqrt{f'_c}$ MPa.

emphasized that this reduction of tensile stress to $0.8f_y$ is not proposed by the code provisions in usual practical design works. Also, it is obvious that reducing the tensile stress by 20% would result in a reduction of both the splice length and the amount of transverse reinforcement over the splices. Consequently, there can be a major deficiency in the behavior of bond strength and ductility response of these lap-spliced concrete beam specimens. Specimen B-14 in the first test series included two continuous tensile bars without lap-spliced bars. This specimen, which was designed based on CSA-A23.3-04, was regarded as a reference specimen with desirable flexural ductility.

With the exception of specimen B-13, which was similar to B-1 but without transverse reinforcement over its splices, for the rest of specimens, transverse reinforcement was calculated by eq. (5) and used along their splices. Specimens B-1 to B-12 in the test series I were divided into two groups having two different tensile nominal bar diameters of 20 mm and 25 mm, respectively. The first group included 6 specimens from B-1 to B-6 with 20 mm nominal diameter bars and the second group included 6 specimens named B-7 to B-12 with 25 mm nominal diameter bars. Each group comprised of three pairs of specimens, i.e., specimen pairs (B-1, B-2), (B-3, B-4), (B-5, B-6) in group 1 and (B-7, B-8), (B-9, B-10), (B-11, B-12) in group 2. The only variable in the specimens of each pair was the size of transverse reinforcing bars, although the ratio of this transverse reinforcement over the splice length, A_t/s, in these specimens was kept constant. The tensile bars were not spliced in specimen B-14 so that it could fail in a flexural mode, with appropriate ductility. The ductility of this specimen was used as a basis to evaluate the ductility of other specimens.

Specimens for the second test series (B-15 to B-22) were selected to propose a design procedure for splice lengths. To prevent bond failure before tensile bar yielding and to ensure a ductile behavior, ACI Committee 318 (1995) Code uses the value of $1.25f_y$ for the bar tensile stress in the splice length calculation. In this study, for the second test series (B-15 to B-22), the two values of either f_y or $1.3f_y$ for the bar tensile stress have been used for splice length calculation. The test results show that the specimens with these values failed after yielding of the reinforcing bars. These tensile stresses would theoretically result in splice lengths for the beams with adequate flexural strength and ductility. The variable parameters in specimens of this test series were the concrete compressive strength, tensile bar size, and the presumed tensile bar stress (i.e., f_y or $1.3f_y$) for the splice length calculation.

Loading

Two concentrated loads were applied to the specimen by means of a hydraulic jack and a spreader beam. A load cell was placed directly under the hydraulic jack and on the top of the spreader beam to transfer the load increments to a data logger acquisition system. A linear variable displacement transducer (LVDT) was placed at the centre of the specimen to transfer the mid-span displacements to the data logger. The load increments and the corresponding displacements were read directly on the data logger. The force–displacement curves were plotted and the ductility for each specimen was investigated. The crack growth of the specimens during loading and at the time of failure was monitored. The duration of each test was approximately 30 min.

Experimental results

Crack growth and failure mode of specimens

Figure 3 shows the crack growth and failure of three specimens in series I and II. All specimens in series I (like specimens B-11 and B-13 in Fig. 3) failed in bond by splitting of the concrete cover over the lap-spliced bars after small displacement, as expected. The exception was specimen B-14 in which the tensile reinforcement was not spliced. This specimen failed in a ductile manner by bending after tensile bars yielding and large displacement. Failure of specimen B-13 which had no transverse reinforcement within the spliced bars was sudden and accompanied by a loud noise. Other specimens failed gradually with relatively large displacements. All specimens in series II failed by yielding of the tensile bars after large displacements (like specimen B-19 in Fig. 3), similar to the specimen B-14 without spliced bars.

Bond strength of specimens

In this section, the experimental bond strength (u_{test}) is compared with the bond strength calculated by eq. (7) (u_{Esf}) and the CSA-A23.3-04 provisions (u_{CSA}) (eqs. (9) and (10)), respectively. The test value, u_{test} is calculated by eq. (11) as follows:

$$u_{test} = \frac{A_b f_s}{\pi d_b l_d} \tag{11}$$

Since in the splice length calculation of series I specimens by eq. (3), the tensile bar stress was considered as $0.8\ f_y$, and the longitudinal bar ratio $\rho = A_s/bd$ (Table 2) in beam sections was less than the maximum ratio ρ_{max}, the elasto-plastic analysis for RC flexural sections could be used to estimate the stresses in the bars at the time of failure. For the calculation of the longitudinal bar ratio within the spliced bars region, the area of the reinforcing bars, A_s, is not doubled because of the splices. This solution, which has been verified by strain gage readings of reinforcing bars, has been used by researchers (Azizinamini et al. 1999*a*; Esfahani and Rangan 1998*b*). Based on the elasto-plastic analysis, the concrete compressive stress distribution in the compressive zone of the sections is almost linear and the tensile bar stress can be calculated by eq. (12) as follows:

$$f_s = \frac{M_{test}}{A_s jd} \tag{12}$$

where M_{test} is the maximum bending moment at failure ($M_{test} = 0.9P_{test}/2$) and jd is the moment lever arm. The parameter j is calculated based on the elasto-plastic analysis (Table 2). Table 3 presents a summary of the test results including the ultimate loads (column 4), ultimate bond stresses (column 6), and the ductility ratios (column 13) for different test specimens. Also, the predicted bond stress values based on eq. (7) and CSA-A23.3-04 (eqs. (9) and (10)) are given in columns 7 and 8, respectively. Columns 9 and 10 compare the test results with the predicted values. As shown in column 4 of Table 3, P_{test} for specimens B-1 and B-13 are 130 and 89 kN, respectively. Specimens B-1 and B-13 are similar except that specimen B-1 was reinforced with appropriate transverse reinforcement along the splice length based on eq. (5). Specimen B-13 had no transverse reinforcement. The ultimate load values of these specimens show that by providing the transverse reinforcement (D8@38 mm) calculated by eq. (5) over the splice length (specimen B-1), the bond strength increases by a factor of 1.5 compared to the similar specimen (B-13) without transverse reinforcement along its splices. In the spliced-beam specimens of series I, the tensile stress of the reinforcing bars f_s was less than the yield stress f_y. Therefore, the term ductility ratio cannot be used for these specimens. For these specimens, the ratio of i is in fact a deformability ratio $\Delta_{0.85}/\Delta_c$ that can be estimated from the load–displacement relationship of the specimens. In this case, Δ_c corresponds to the intersection of the tangents to the load–displacement curve at the origin and maximum displacement, Δ_{max}. As shown in column 13 of Table 3, the deformability of specimen B-1 ($i = \Delta_{0.85}/\Delta_c = 2.32$) is relatively high compared to that of specimen B-13 ($i = \Delta_{0.85}/\Delta_c = 1.15$). These values of deformability ratios as well as the strength ratios in column 10 show the beneficial effect of transverse reinforcement in improving the strength and deformation capacity of flexural beams with spliced bars. It can

Fig. 3. Crack growth and failure state of three specimens in series I and II.

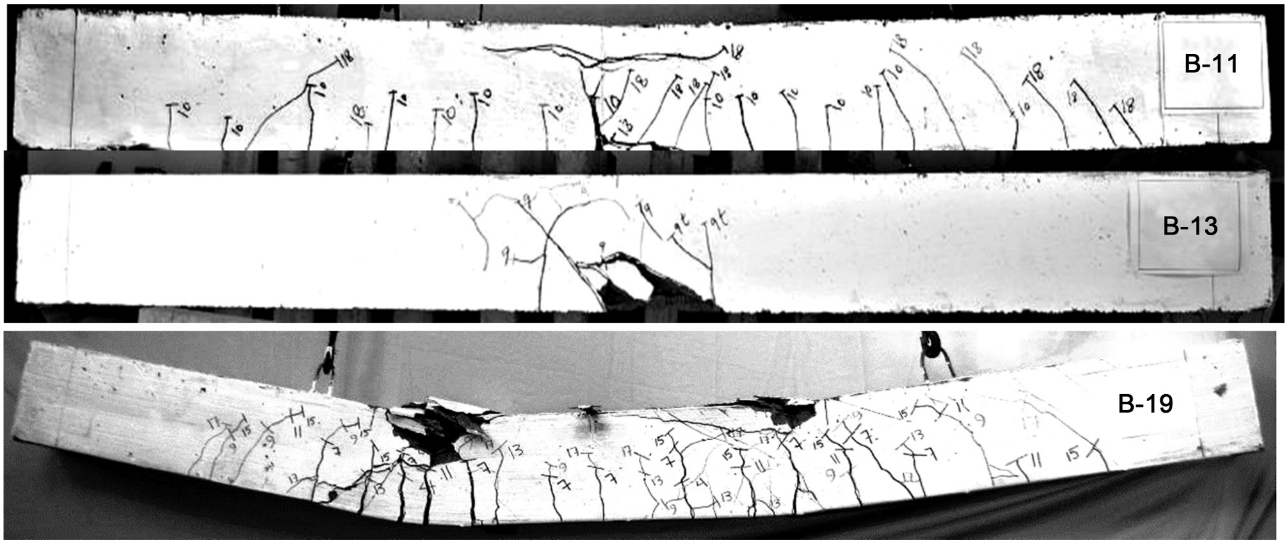

Table 3. Summary of test results.

Series	Specimen number [1]	d_b (mm) [2]	f'_c (MPa) [3]	P_{test} (kN) [4]	f_s (MPa) [5]	u_{test} (MPa) [6]	u_{Esf} [7]	u_{CSA} [8]	$\frac{u_{test}}{u_{Esf}}$ [9]	$\frac{u_{test}}{u_{CSA}}$ [10]	Δ_c (mm) [11]	$\Delta_{0.85}$ (mm) [12]	$i = \frac{\Delta_{0.85}}{\Delta_c}$ [13]
I	B-01	22	24	155	413	4.63	4.12	2.12	1.13	2.22	17.6	38.0	2.15
	B-02	22	24	143	383	4.29	4.12	2.12	1.05	2.04	16.5	32.0	1.95
	B-1	20	22	130	410	5.16	4.77	2.54	1.07	2.01	12.8	29.7	2.32
	B-2	20	22	121	382	4.80	4.77	2.54	0.99	1.87	14.6	26.4	1.81
	B-3	20	45	144	448	8.55	6.99	3.63	1.19	2.31	14.4	27.5	1.91
	B-4	20	45	143	446	8.51	6.99	3.63	1.19	2.3	13.9	22.0	1.60
	B-5	20	70	144	443	10.65	11.34	4.52	0.91	2.27	16.0	21.7	1.35
	B-6	20	70	133	409	9.83	11.34	4.52	0.84	2.1	19.2	25.4	1.32
	B-7	25	22	166	346	4.21	4.31	2.03	0.99	2.1	11.8	20.9	1.80
	B-8	25	22	163	340	4.15	4.31	2.03	0.97	2.07	14.5	23.0	1.60
	B-9	25	45	175	360	6.66	6.31	2.9	1.06	2.3	14.0	22.5	1.60
	B-10	25	45	174	358	6.61	6.31	2.9	1.05	2.28	16.9	25.1	1.50
	B-11	25	70	179	364	8.50	10.05	3.62	0.84	2.32	17.4	21.5	1.25
	B-12	25	70	174	353	8.25	10.05	3.62	0.81	2.25	19.7	24.3	1.23
	B-13	20	22	89	280	3.53	4.04	2.54	0.86	1.37	8.90	10.3	1.15
	B-14	20	22	140	446	—	—	—	—	—	18.7	41.2	2.21
	Mean								**1.00**	**2.12**	—		
	SD								**0.12**	**0.24**	—		
II	B-15	20	31	161	501>460	6.83	5.70	3.01	1.20	2.27	17.2	120.4	7.00
	B-16	25	31	245	540>420	6.02	5.10	2.41	1.18	2.5	20.9	82.9	3.97
	B-17	20	74	182	518>460	11.86	8.72	4.65	1.36	2.55	22.2	83.0	3.74
	B-18	25	74	255	492>420	9.58	7.85	3.72	1.22	2.57	22.2	64.0	2.88
	B-19	20	31	175	548>460	5.94	5.17	3.01	1.15	1.97	16.7	177.0	10.60
	B-20	25	31	245	541>420	4.83	4.69	2.41	1.03	2.01	19.7	45.3	2.30
	B-21	20	74	183	519>460	9.48	7.90	4.65	1.20	2.04	21.2	143.0	6.75
	B-22	25	74	253	489>420	7.61	7.18	3.72	1.06	2.05	21.7	58.0	2.67
	Mean								**1.18**	**2.24**	—		
	SD								**0.10**	**0.26**	—		
All	**Mean**								**1.06**	**2.18**	—		
	SD								**0.14**	**0.26**	—		

Note: SD, standard deviation.

also be seen in column 9 of Table 3 that the average and the standard deviation of the ratio u_{test}/u_{Esf} for all specimens in series I are 1.00 and 0.12, respectively. These values indicate that the bond strength can be estimated with a good accuracy by using eq. (7) for different concrete compressive strengths and different amounts of the transverse reinforcement over the splices of the beams. However, as shown in column 10 of Table 3, the average and standard deviation for the u_{test}/u_{CSA} ratio of all specimens in series I are 2.12 and 0.24, respectively. Therefore, CSA-A23.3-04 Code predicts the flexural strength of beams with spliced bars with a large scatter.

Deformability and ductility of specimens

The load versus mid-span displacement curves of all specimens in series I and II are represented in Figs. 4 and 5, respectively. Also, the displacements of $\Delta_{0.85}$ and Δ_y of all specimens are shown in these figures. As seen in Fig. 4 and Table 3, the values of $\Delta_{0.85}$ and Δ_y of the specimen B-13 (without transverse reinforcement over its

Fig. 4. Bond strength and ductility of different specimens in series I.

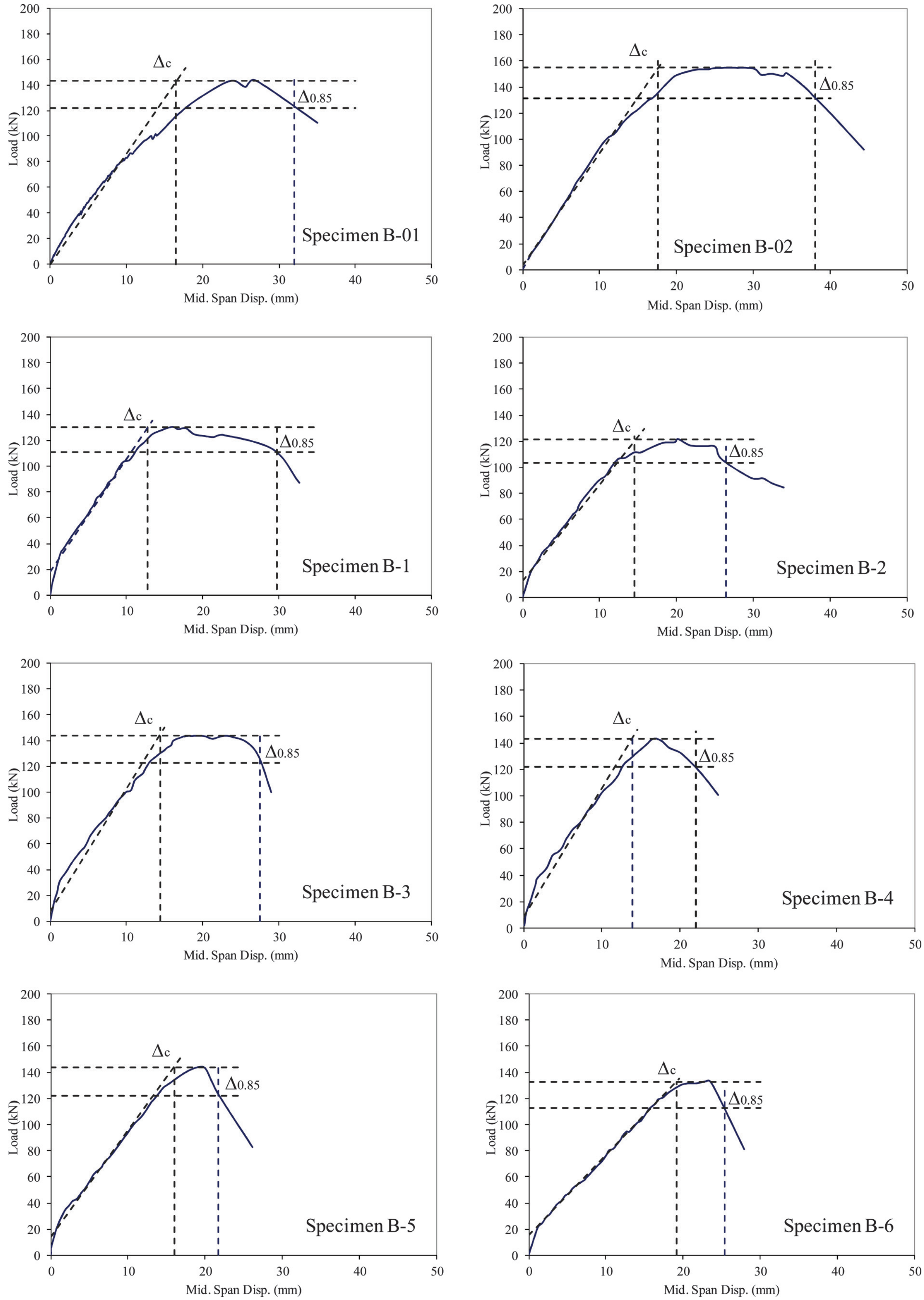

Fig. 4 (*concluded*).

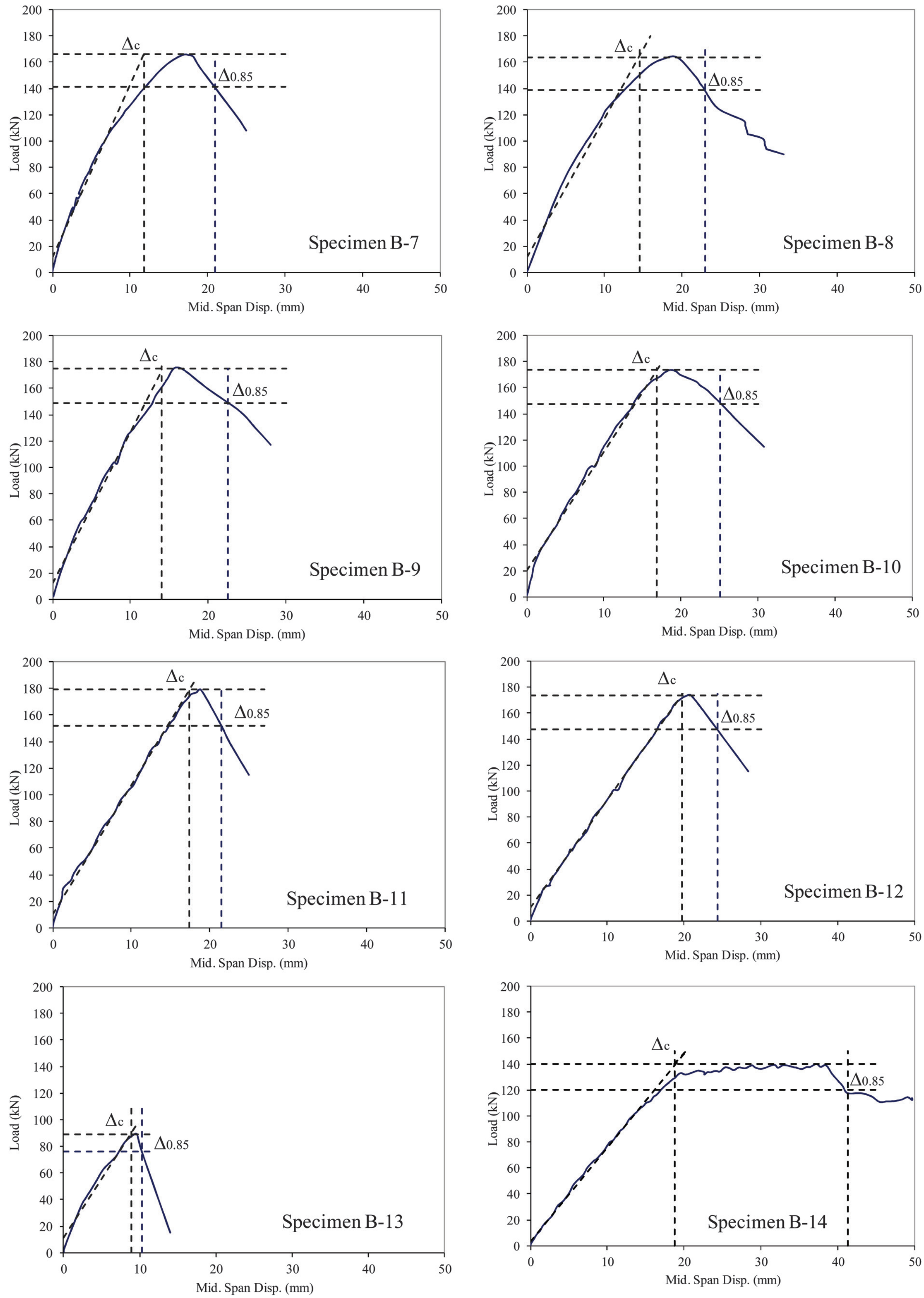

Fig. 5. Bond strength and ductility of different specimens in series II.

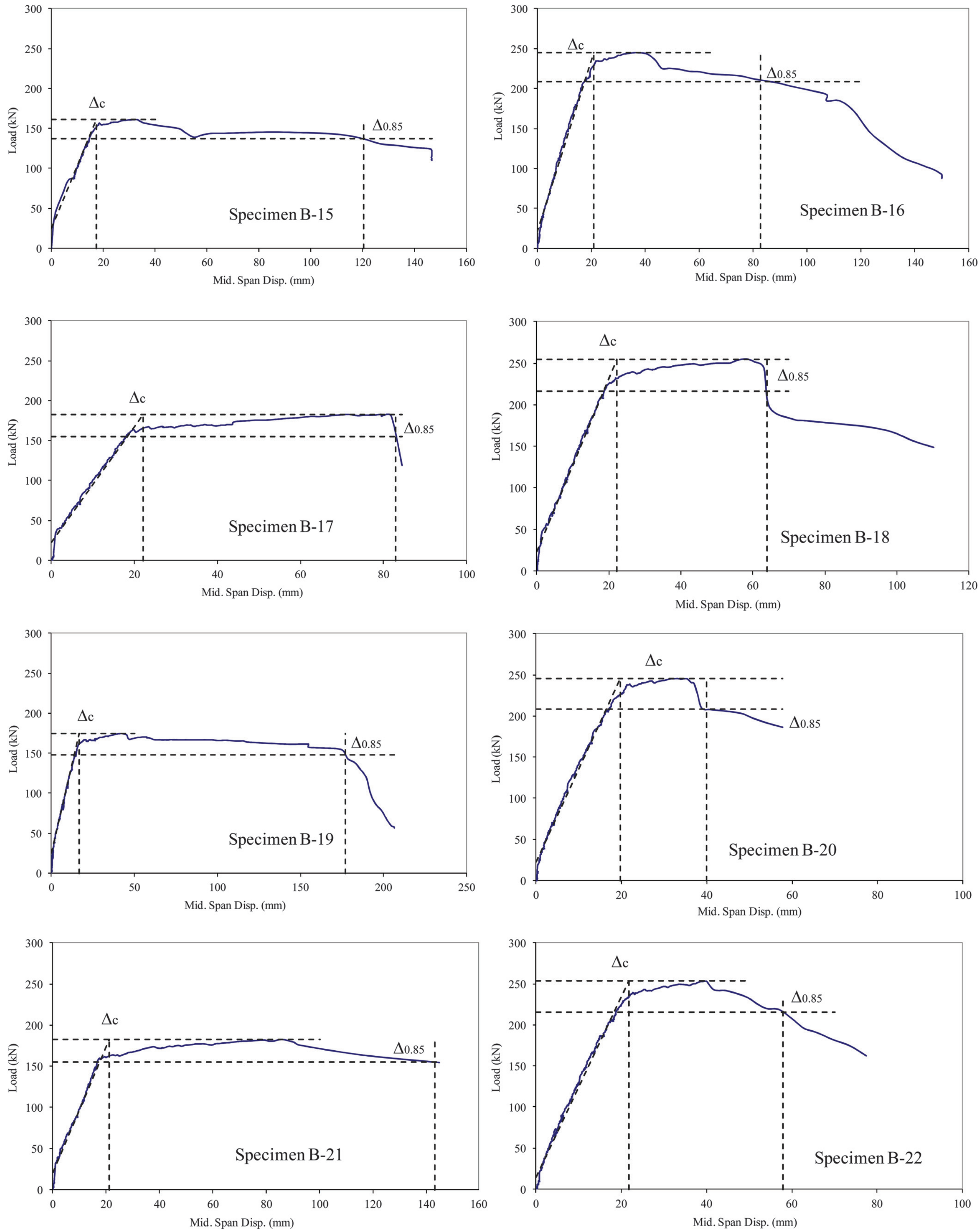

splices) are very close to each other and its deformability ratio is about 1.15 (column 13, Table 3), which indicates that this specimen lacks deformability. The increase of the deformability ratio of the specimens with spliced bars is not due to the bar yielding, but because of the slip of the spliced bars. Specimen B-13 failed by splitting in the extreme tension fibre in a very brittle manner. Other specimens had appropriate transverse reinforcement over their splice lengths and their deformability ratios are larger than that of specimen B-13 (Table 3 and Fig. 4).

Specimen B-14, in which the tensile bars were not spliced, was used as a reference to evaluate the ductility of other specimens. Specimen B-14 shows a more ductile behavior and the rate of the strength decay is not as severe as the other specimens in series I. The ductility ratio of specimen B-14 is controlled by the reinforcing bar yielding. Based on the CSA-A23.3-04 provisions, this specimen was under-reinforced ($c/d < 700/(700 + f_y)$ which is equivalent to $\rho < \rho_{max}$) and thus flexurally ductile, where c/d is the neutral axis depth over effective depth ratio in beams. As seen in Fig. 4 and Table 3, the displacement ductility ratio for this specimen is estimated as 2.2 ($\Delta_{0.85}/\Delta_c = 41.2/18.7 = 2.2$).

The ductility ratios of series II specimens are much higher than that of the reference specimen B-14 ($i = 2.2$) without spliced bars. This is because of the large slip of the spliced bars confined by adequate transverse reinforcement (i.e., the ductility ratio of series II specimens is not only controlled by reinforcing bar yielding but also by slip of the spliced bars in the spliced bars region, thus it is larger than the ductility ratio of specimen B-14). In the reference specimen, the reinforcing bars are not spliced, thus the slip is limited.

As mentioned earlier, the splice length and the amount of transverse reinforcement over the splices of series I specimens were reduced due to considering the tensile stress of the longitudinal bars as 80% of the yield stress (to ensure that failure occurs in bond mode). This reduction was not used in series II specimens. To prevent bond failure before yielding of tensile bars and to ensure a ductile behavior, ACI Committee 318 (1995) Code uses the value of $1.25f_y$ for the bar tensile stress in the splice length calculation. For the test series II, the splice length calculation was based on the reinforcing bar stress of either f_y or 1.3 f_y. The reinforcing bar stresses of the specimens in this test series were initially calculated based on the ultimate strength method without considering the yield stress values of the reinforcing bars (column 5 in Table 3). Then the reinforcing bar stresses were compared with the yield stress values. The calculated stresses of the reinforcing bars in the column 5 of Table 3 are larger than the yield stresses of different reinforcing bars in the specimens of series II. These large stress values together with the load–displacement relationships of the specimens in test series II and the failure modes indicate that these specimens had failed after yielding of the spliced bars (with adequate flexural strength and ductility). Therefore, for these specimens, bond stresses in column 6 were calculated using the yield stresses of the bars but not the calculated values given in column 5 of Table 3.

Column 13 of Table 3 and Fig. 5 present the ductility ratios of series II specimens which show values ranging between 2.3 and 10.6. The ductility ratios of series II specimens are much higher than that of the reference specimen B-14 ($i = 2.2$) without spliced bars. This is mainly because of the large slip of the spliced bars confined by adequate transverse reinforcement in the specimens in series II. As mentioned earlier, specimen B-14 as well as the specimens in the test series II satisfied the flexural ductility requirements of CSA-A23.3-04.

Comparison between test results and predicted bond strength values

Table 3 summarizes the test results and the comparisons of the bond strength values between test results and the predicted values by CSA-A23.3-04 Code and the equations proposed by Esfahani and Kianoush (2005). By comparing the values of u_{test}/u_{Esf} and u_{test}/u_{CSA} in columns 9 and 10 of Table 3, for different beam parameters and concrete strengths, the prediction of the equations by Esfahani and Kianoush (2005) in terms of the mean value and standard deviation of the results is very satisfactory. As seen in the column 9 of Table 3, the mean value and the standard deviation of the ratio u_{test}/u_{Esf} for all specimens of series I and II are 1.06 and 0.14, respectively. These values indicate that the bond strength can be estimated with a good accuracy by using eqs. (3), (5), and (7) for different concrete compressive strengths and different amounts of the transverse reinforcement over the splices of the beams. In comparison, the mean value and the standard deviation of the ratio u_{test}/u_{CSA} for all specimens are 2.18 and 0.26, respectively.

Effect of transverse reinforcement on bond strength and ductility

The ductility and bond strength of the two similar specimens B-1 and B-13 with and without transverse reinforcement over the splice length can be compared with those of specimen B-14 in Fig. 4. As mentioned previously, B-14 is considered a ductile specimen based on the CSA-A23.3-04 provisions for flexural beams. Figure 4 shows the load–displacement response of specimen B-1, in which the transverse reinforcement (D8@38 mm) was calculated by eq. (5), is close to that of specimen B-14. However, specimen B-13 failed in a very brittle and violent manner without exhibiting ductility.

The effect of transverse reinforcement spacing (s) over the splice length can be investigated in specimens B-1 to B-12. Each pair of similar specimens (B-1, B-2), (B-3, B-4), (B-5, B-6), (B-7, B-8), (B-9, B-10), and (B-11, B-12) have a constant value of A_t/s, but with different transverse bar diameters and spacing. A comparison of bond strength and ductility of these specimens shows that using transverse reinforcing bars with a smaller bar diameter and spacing results in a higher ductility (Fig. 4). Column 13 of Table 3 presents the ductility ratio values of these specimens.

Effect of concrete compressive strength on bond strength and ductility

The load–displacement responses for three similar specimens B-1, B-3, and B-5 with different concrete compressive strengths of 22, 45, and 70 MPa, respectively, are shown in Fig. 4. The ductility ratios of these specimens are also given in column 13 of Table 3. It is seen that with increasing the concrete compressive strength, the bond strength increases and the ductility ratio decreases. Specimen B-1 with concrete compressive strength of 22 MPa shows the most satisfactory response in terms of displacement–ductility ratio (the ductility ratio of this specimen is 2.32, which is more than that of the reference specimen B-14 with a value of 2.21.). The ductility of specimen B-3 with 45 MPa is also satisfactory (its ductility ratio is 1.91, not much lower than the reference value, 2.21.), but for that of specimen B-5 with concrete compressive strength of 70 MPa is rather low (with a ductility ratio of 1.35, which is significantly lower than the reference value, 2.21). Similar observation was reported by Pessiki and Pieroni (1997) in high strength concrete columns in which, for obtaining similar ductility, larger tie-bars were needed when the concrete strength increased.

Likewise, the effect of increasing concrete compressive strength on the reduction of displacement–ductility ratio may also be verified for the three similar specimens B-7, B-9, and B-11 with concrete compressive strengths of 22, 45, and 70 MPa, respectively. The ductility ratio for specimen B-11 with concrete compressive strength of 70 MPa is 1.25 (smaller than 1.80) and 1.60 for specimens B-7 and B-9, respectively (Table 3).

For test series II in which the splice lengths were determined by eq. (3) using reinforcing bar tensile stress f_s equal to f_y or 1.3 f_y, the ductility ratio for all specimens was more than the reference value of 2.21. As seen in column 13 of Table 3 and Fig. 5, for these specimens, the ductility ratios are between 2.3 and 10.6. Similar to series I specimens, the effect of increasing concrete compressive strength on the reduction of displacement–ductility ratio is also seen in series II specimens.

Conclusion

The objective of this research study was to investigate the bond strength and ductility of lap-spliced RC beams. Twenty-four beam specimens were manufactured and tested. A comparison of the test results was carried out with the equations proposed by Esfahani and Kianoush (2005) and also CSA-A23.3-04 Standard provisions to investigate the effects of different parameters on bond strength and ductility of specimens. Based on the test results, the following conclusions were drawn.

1. The efficiency of the proposed equations for the computations of bond strength of lap-spliced RC beams was assessed by the test results and it was found that the accuracy of the equations is quite satisfactory. For all test results in this study, the average of the test over calculated bond strength ratios is 1.06 with a standard deviation of 0.14. Using the current CSA-A32.3 equation, these values are 2.18 and 0.26, respectively.
2. Based on the test results of this study, the current CSA-A23.3-04 Standard equation predicts the bond strength of lap-spliced concrete beams, conservatively. However, it cannot guarantee to achieve a satisfactory ductility for these beams because it does not require transverse reinforcement over the splice length. It seems logical that the provisions of this Standard should be revised appropriately, so that a satisfactory ductility criterion could be achieved.
3. Based on the assumption of yield stress for the tensile reinforcing bar, the previously proposed equations as mentioned above were used for designing the splice length and the required transverse reinforcement. On this basis, a series of spliced-beam specimens were designed and manufactured. Using the test results of these specimens, it was shown that the application of the proposed equations for the calculation of splice length and the amount of transverse reinforcement over the splice length resulted in satisfactory solutions for the bond strength and ductility of RC beams for different concrete strengths.
4. Although it is found that a certain minimum amount of transverse reinforcement is needed to achieve a satisfactory ductility response for lap-spliced RC beams, the test results show that using smaller stirrup sizes and spacing results in a better ductility response.

References

ACI Committee 318. 1995. Building code requirements for reinforced concrete and commentary. American Concrete Institute (ACI), Detroit. 369 pp.

Aly, R. 2007. Stress along tensile lap-spliced fiber reinforced polymer reinforcing bars in concrete. Canadian Journal of Civil Engineering, **34**(9): 1149–1158. doi:10.1139/l07-046.

Azizinamini, A., Pavel, R., Hatfield, E., and Gosh, S.K. 1999*a*. Behavior of lap-spliced reinforcing bars embedded in high strength concrete. ACI Structural Journal, **96**(5): 826–836. doi:10.14359/737.

Azizinamini, A., Darwin, D., Eligehausen, R., Pavel, R., and Ghosh, S.K. 1999*b*. Proposed modifications to ACI 318-95 tension development and lap splice for high-strength concrete. ACI Structural Journal, **96**(6): 922–927. doi:10.14359/766.

Cohn, M.Z., and Bartlett, M. 1982. Computer-simulated flexural tests of partially pre-stressed concrete sections. ASCE Journal of Structural Division, **108**(ST12): 2747–2765.

CSA-A23.3-04. 2004. Design of concrete structures. CAN/CSA A23.3, Canadian Standards Association (CSA), Rexdale, Ont.

Esfahani, M.R. 2000. Behavior of lap-spliced reinforcing bars embedded in high-strength Concrete paper by Azizinamini et al. Discussion, ACI Structural Journal, **97**(4): 669–670.

Esfahani, M.R., and Kianoush, M.R. 2005. Development/splice length of reinforcing bars. ACI Structural Journal, **102**(1): 22–30. doi:10.14359/13527.

Esfahani, M.R., and Rangan, B.V. 1998*a*. Local bond strength of reinforcing bars in normal strength and high-strength concrete (HSC). ACI Structural Journal, **95**(2): 96–106.

Esfahani, M.R., and Rangan, B.V. 1998*b*. Bond between normal strength and high-strength concrete (HSC) and reinforcing bars in splices in beams. ACI Structural Journal, **95**(3): 272–280. doi:10.14359/545.

Esfahani, M.R., and Rangan, B.V. 2000. Influence of transverse reinforcement on bond strength of tensile splices. Cement and concrete composites, **22**: 159–163. doi:10.1016/S0958-9465(00)00005-6.

Orangun, C.O., Jirsa, J.O., and Breen, J.E. 1977. Reevaluation of test data on development length and splices. ACI Journal, Proceedings, **74**(3): 114–122.

Pessiki, S., and Pieroni, A. 1997. Axial load behavior of large-scale spirally-reinforced high strength concrete columns. ACI Structural Journal, **94**(3): 304–314. doi:10.14359/482.

Rezansoff, T., Zhang, S., and Sparling, B.F. 1997. Influence of different stirrup configurations on lap splices in beams. Canadian Journal of Civil Engineering, **24**(1): 106–114. doi:10.1139/l96-094.

Tepfers, R. 1973. A theory of bond applied to overlapped tensile reinforcement splices for deformed bars. Chalmers TekniskaHoegskola Publication 73.2, Division of Concrete Structures, Chalmers University of Technology, Gothenburg, Sweden, 328 pp.